ISSN 0005-1179 (print), ISSN 1608-3032 (online), Automation and Remote Control, 2026, Vol. 87, No. 6, pp. 510–518.

Assessment of the Feasibility of Intercepting an Intensively Maneuvering High-Speed Aircraft by an Inertial Interceptor with a Time-Varying Control Law

V. S. Verba[*,a], **V. I. Merkulov**[*,b], **and D. V. Zakomoldin**[**,c]

[*] *JSC Concern Vega, Moscow, Russia*
[**] *Military Academy of Aerospace Defense named after Marshal of the Soviet Union G.K. Zhukov, Tver, Russia*
e-mail: [a] *vvs.msk@gmail.com,* [b] *ilya-zagrebelnyi@mail.ru,* [c] *denjuga68@yandex.ru*

Received July 30, 2025
Revised October 10, 2025
Accepted October 15, 2025

Abstract—This paper presents a time-varying control law designed for an interceptor's guidance to an intensively maneuvering aircraft (aerial target). The control law takes into account the mismatch between the dynamic properties of the interceptor and the target. Simulation results are provided, indicating the potential feasibility of intercepting the target and improving guidance accuracy.

Keywords: interceptor control law, maneuvering aerial target, mismatch of dynamic properties, miss distance

DOI: 10.7868/S1608303226060036

1. INTRODUCTION

An effective solution of the problem of intercepting aerospace attack means is necessitated by the requirement to protect important objects of the defending side from potential destruction.

In view of the continuous improvement trend of aerospace attack means toward increasing their speed and maneuverability characteristics [1–7], the inertia of interceptors can be a significant factor affecting their potentially achievable guidance performance to an intensively maneuvering high-speed aircraft (HSA) [8].

Two possible approaches to considering the interceptor's inertia were discussed in [8]. The first approach is to generate a control signal based on the predicted rather than current values of the HSA state coordinates. The second approach involves an appropriate transformation of input actions that compensates for the interceptor's inertia via control signal corrections covering high derivatives of the state coordinates. However, these approaches complicate the information support system due to the need to estimate high derivatives of the line-of-sight (LoS) angular rate [8].

Therefore, it is topical to design alternative control signals for an interceptor's guidance to an HSA with the following requirements [9]:

—The control signal should take into account the mismatches between the dynamic properties of the interceptor and HSA.

—The control signal should be time-varying to redistribute control priorities from eliminating angle guidance errors at the initial guidance stage to eliminating the LoS angular rate when approaching the HSA.

This paper aims to design a time-varying control signal for an inertial interceptor with the potential feasibility of intercepting an HSA.

2. PROBLEM STATEMENT. CONTROL SIGNAL DESIGN

The design procedure is based on the local optimization approach of the statistical theory of optimal control (STOC) within the linear-quadratic-Gaussian problem framework. For a given system described by [9]

$$\dot{\mathbf{x}}(t) = \mathbf{F}(t)\mathbf{x}(t) + \mathbf{B}\mathbf{u}(t) + \xi(t), \tag{1}$$

which includes a subsystem (aerial target) of the form

$$\dot{\mathbf{x}}_{\text{tar}}(t) = \mathbf{F}_{\text{tar}}(t)\mathbf{x}_{\text{tar}}(t) + \xi_{\text{tar}}(t), \tag{2}$$

generating input actions for another subsystem (interceptor)

$$\dot{\mathbf{x}}_{\text{int}}(t) = \mathbf{F}_{\text{int}}\mathbf{x}_{\text{int}}(t) + \mathbf{B}_{\text{int}}\mathbf{u}(t) + \xi_{\text{int}}(t), \tag{3}$$

under available measurements

$$\mathbf{z}(t) = \mathbf{H}\mathbf{x}(t) + \xi_{\text{z}}(t), \tag{4}$$

this approach yields the optimal control law

$$\mathbf{u}(t) = \mathbf{K}^{-1}\mathbf{B}_{\text{int}}^T\left[\mathbf{Q}\Delta\hat{\mathbf{x}}(t) - \mathbf{G}\hat{\mathbf{s}}_{\text{int}}(t)\right], \tag{5}$$

in terms of the minimum value of the performance functional

$$\begin{aligned} I = M\Bigg\{ &(\mathbf{x}_{\text{tar}}(t) - \mathbf{x}_{\text{int}}(t))^T\mathbf{Q}(\mathbf{x}_{\text{tar}}(t) - \mathbf{x}_{\text{int}}(t)) + 2(\mathbf{x}_{\text{tar}}(t) - \mathbf{x}_{\text{int}}(t))^T\mathbf{G}\mathbf{s}_{\text{int}}(t) \\ &+ \mathbf{s}_{\text{int}}^T(t)\mathbf{Q}\mathbf{s}_{\text{int}}(t) + \int_0^t \mathbf{u}^T(t)\mathbf{K}\mathbf{u}(t)\,dt \Bigg\}, \end{aligned} \tag{6}$$

where

$$\begin{gathered} \mathbf{x} = \begin{bmatrix}\mathbf{x}_{\text{tar}}^T & \mathbf{x}_{\text{int}}^T\end{bmatrix}^T, \quad \mathbf{F} = \begin{bmatrix}\mathbf{F}_{\text{tar}} & \mathbf{O}_1 \\ \mathbf{O}_2 & \mathbf{F}_{\text{int}},\end{bmatrix}, \quad \mathbf{B} = \begin{bmatrix}\mathbf{O}_3\mathbf{B}_{\text{int}}\end{bmatrix}, \quad \mathbf{s}_{\text{int}} = \left(\mathbf{F}_{\text{tar}} - \mathbf{F}_{\text{int}}\right)\mathbf{x}_{\text{tar}}, \\ \xi = \begin{bmatrix}\xi_{\text{tar}}^T & \xi_{\text{int}}^T\end{bmatrix}^T, \quad \Delta\hat{\mathbf{x}} = \hat{\mathbf{x}}_{\text{tar}} - \hat{\mathbf{x}}_{\text{int}}, \end{gathered} \tag{7}$$

The other designations are as follows: $\mathbf{x}_{\text{int}}$ and $\mathbf{x}_{\text{tar}}$ are the n-dimensional state vectors of the interceptor and target, respectively; $\mathbf{F}_{\text{int}}$ and $\mathbf{F}_{\text{tar}}$ are the internal connection matrices of the subsystems (2) and (3), characterizing their dynamics; $\mathbf{u}$ is the control vector; $\mathbf{B}_{\text{int}}$ is the control efficiency matrix; $\mathbf{z}$ is the measurement vector; ξ is the noise vector; ξ_{tar}, ξ_{int}, and ξ_z are the noise vectors of the states (2), (3) and measurements (4), respectively; $\mathbf{H}$ is the connection matrix between $\mathbf{z}$ and $\mathbf{x}$; $\mathbf{Q}$ and $\mathbf{K}$ are nonnegative definite penalty matrices for control accuracy and control costs, respectively; $\mathbf{G}$ is the mutual connection matrix between $\Delta\mathbf{x}$ and $\mathbf{s}_{\text{int}}$; $\mathbf{s}_{\text{int}}$ is the mismatch vector between the dynamic properties of the subsystems; t is the current time; $\mathbf{O}_1$–$\mathbf{O}_3$ are zero matrices of compatible dimensions; finally, $M\{\bullet\}$ denotes the expectation operator.

To shorten the mathematical derivations, the dependence on time in (1)–(7) will be omitted.

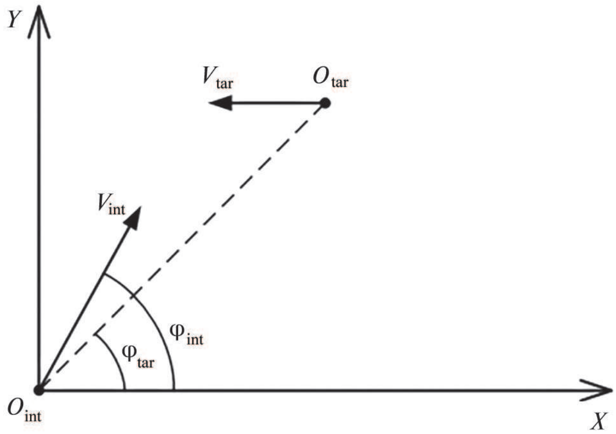

Fig. 1. The mutual arrangement of the target and interceptor.

The geometry of the target's and interceptor's angles is shown in Fig. 1. In this figure, O_{int} and O_{tar} are the positions of the interceptor and target, respectively; $\mathbf{V}_{\text{tar}}$ and $\mathbf{V}_{\text{int}}$ are the velocity vectors of the target and interceptor, respectively; φ_{int} is the interceptor's line-of-sight (LoS) angle (the angle between its velocity vector and the horizontal axis); finally, φ_{tar} is the HSA's flight direction angle (the angle between the interceptor–target LoS and the horizontal axis).

The control design problem is formulated as follows.

Let an HSA (target) be described by a system of equations of the form:

$$\begin{aligned}
&\dot{\varphi}_{\text{tar}} = \omega_{\text{tar}}, && \varphi_{\text{tar}}(0) = \varphi_{\text{tar}0},\\
&\dot{\omega}_{\text{tar}} = -\frac{2\dot{R}}{R}\omega_{\text{tar}} + \frac{1}{R}(j_{\text{tar}} - j_{\text{int}}) + \xi_{\text{tar}}, && \omega_{\text{tar}}(0) = \omega_{\text{tar}0}.
\end{aligned} \tag{8}$$

For an inertial interceptor corresponding to the model

$$\begin{aligned}
&\dot{\varphi}_{\text{int}} = \omega_{\text{int}}, && \varphi_{\text{int}}(0) = \varphi_{\text{int}0},\\
&\dot{\omega}_{\text{int}} = -\frac{1}{T_{\text{int}}}\omega_{\text{int}} + \frac{b}{T_{\text{int}}}j_{\text{int}} + \xi_{\text{int}}, && \omega_{\text{int}}(0) = \omega_{\text{int}0},
\end{aligned} \tag{9}$$

with available measurements of the form

$$\varphi_z = \varphi_{\text{tar}} + \xi_z, \tag{10}$$

it is required to find a control signal j_{int} minimizing the performance functional

$$\begin{aligned}
I = M\Bigg\{ &\begin{bmatrix}\varphi_{\text{tar}} - \varphi_{\text{int}}\\ \omega_{\text{tar}} - \omega_{\text{int}}\end{bmatrix}^T \begin{bmatrix}\dfrac{q_{11}}{R} & q_{12}\\ q_{21} & \dfrac{q_{22}}{R}\end{bmatrix} \begin{bmatrix}\varphi_{\text{tar}} - \varphi_{\text{int}}\\ \omega_{\text{tar}} - \omega_{\text{int}}\end{bmatrix}\\
&+ 2\begin{bmatrix}\varphi_{\text{tar}} - \varphi_{\text{int}}\\ \omega_{\text{tar}} - \omega_{\text{int}}\end{bmatrix}^T \begin{bmatrix}g_{11} & g_{12}\\ g_{21} & g_{22}\end{bmatrix} \begin{bmatrix}0\\ \left(\dfrac{1}{T_{\text{int}}} - \dfrac{2\dot{R}}{R}\right)\omega_{\text{tar}}\end{bmatrix}\\
&+ \begin{bmatrix}0\\ \left(\dfrac{1}{T_{\text{int}}} - \dfrac{2\dot{R}}{R}\right)\omega_{\text{tar}}\end{bmatrix}^T \begin{bmatrix}\dfrac{q_{11}}{R} & q_{12}\\ q_{21} & \dfrac{q_{22}}{R}\end{bmatrix} \begin{bmatrix}0\\ \left(\dfrac{1}{T_{\text{int}}} - \dfrac{2\dot{R}}{R}\right)\omega_{\text{tar}}\end{bmatrix} + \int_0^t j_{\text{int}}^2 k_{\text{j}}\, dt\Bigg\}.
\end{aligned} \tag{11}$$

The expressions (8)–(11) have the following notation: φ_{tar} and φ_{int} are the target's LoS angle and the interceptor's flight direction angle, respectively, in the frame associated with the interceptor's center of mass; ω_{tar} and ω_{int} are the LoS angular rates of the target and interceptor, respectively; φ_{tar0}, φ_{int0} and ω_{tar0}, ω_{int0} are the initial values of the corresponding angles and their rates, respectively; b and T_{int} are the interceptor's gain and time constant, respectively; j_{tar} and j_{int} are the lateral accelerations of the target and interceptor, respectively; R and $\dot{R}$ are the interceptor's range to the target and its rate of change, respectively; ξ_{tar} and ξ_{int} are the disturbances of the target and interceptor trajectories (centered Gaussian noises); $\frac{q_{11}}{R}$, q_{12}, q_{21}, and $\frac{q_{22}}{R}$ are nonnegative elements of the matrix $\mathbf{Q}$; finally, g_{11}, g_{12}, g_{21}, and g_{22} are nonnegative elements of the matrix $\mathbf{G}$. Note that in practice, the most difficult task is to find the elements of the matrices $\mathbf{Q}$, $\mathbf{G}$, and $\mathbf{K}$; here, the solution is often empirical. The most well-known method involves the principle of equal strength: the products of the squared maximum permissible errors and the corresponding penalty coefficients are supposed to be the same for all coordinates. By setting the maximum permissible errors (variances) and a penalty coefficient for a single coordinate, one can preliminarily estimate the penalty coefficients for the other coordinates. Then the resulting coefficients are refined based on simulation.

The time-varying target model (8) is highly universal due to, first, consideration of the influence of the range and approach speed on the angular coordinates and, second, the realizability of maneuvers of almost any complexity by manipulating the laws of change of j_{tar}.

While being fairly simple, the kinematic models (8) and (9) describe the mutual arrangement (geometry) of the interceptor and HSA and the geometry's rate of change with sufficient accuracy for the problem under consideration [8].

The performance functional (11) possesses the following features. Besides the requirements for control accuracy and control costs (the first and fourth terms of the functional), it covers the requirement to reduce the mutual influence of control errors and the mismatch between the dynamic properties of the interceptor and HSA (the second term), as well as the requirement to compensate for the above mismatch (the third term). In addition, the first and third terms of the performance functional (11) contain the time-varying coefficients of the control accuracy penalty matrix, $\frac{q_{11}}{R}$ and $\frac{q_{22}}{R}$, which yield a time-varying control signal even when using the simplified time-invariant interceptor model (9); for details, see [9].

Models (8) and (9) are linear, the noises are Gaussian, and the performance functional (11) is quadratic. Therefore, based on the separation theorem and the statistical equivalence principle, control signals will be designed using the deterministic models (8) and (9) with $\xi_{\text{tar}} = 0$, $\xi_{\text{int}} = 0$, and the coordinates of (8) and (9) replaced by their optimal estimates.

By matching (8) with (2), (9) with (3), and (11) with (6) and (7), we obtain

$$\begin{gathered}
\mathbf{x}_T = \begin{bmatrix} \hat{\varphi}_{\text{tar}} \\ \hat{\omega}_{\text{tar}} \end{bmatrix}, \quad \mathbf{x}_{\text{int}} = \begin{bmatrix} \hat{\varphi}_{\text{int}} \\ \hat{\omega}_{\text{int}} \end{bmatrix}, \quad \mathbf{B}_{\text{int}} = \begin{bmatrix} 0 \\ \dfrac{b}{T_{\text{int}}} \end{bmatrix}, \quad \mathbf{u} = \hat{j}_{\text{int}}, \\
\mathbf{Q} = \begin{bmatrix} \dfrac{q_{11}}{R} & q_{12} \\ q_{21} & \dfrac{q_{22}}{R} \end{bmatrix}, \quad \mathbf{G} = \begin{bmatrix} g_{11} & g_{12} \\ g_{21} & g_{22} \end{bmatrix}, \quad \mathbf{F}_{\text{int}} = \begin{bmatrix} 0 & 1 \\ 0 & -\dfrac{1}{T_{\text{int}}} \end{bmatrix}, \\
\mathbf{F}_{\text{tar}} = \begin{bmatrix} 0 & 1 \\ 0 & -\dfrac{2\hat{\dot{R}}}{\hat{R}} \end{bmatrix}, \quad \mathbf{s}_{\text{int}} = \begin{bmatrix} 0 \\ \left(\dfrac{1}{T_{\text{int}}} - \dfrac{2\hat{\dot{R}}}{\hat{R}} \right) \hat{\omega}_{\text{tar}} \end{bmatrix}, \quad \mathbf{K} = k_j.
\end{gathered} \tag{12}$$

Based on direct analysis of $\mathbf{s}_{\text{int}}$, we draw the following conclusions: at long ranges (as $\hat{\omega}_{\text{tar}} \to 0$), the mismatch of the dynamic properties of the HSA and interceptor has almost no effect; at short ranges, characterized by an increasing value of $\hat{\omega}_{\text{tar}}$, the significance of $\mathbf{s}_{\text{int}}$ grows gradually.

Substituting (12) into (5) gives

$$\jmath_{\text{int}} = \frac{1}{k_{\text{j}}} \begin{bmatrix} 0 \\ \dfrac{b}{T_{\text{int}}} \end{bmatrix}^T \left[\begin{bmatrix} \dfrac{q_{11}}{\hat{R}} & q_{12} \\ q_{21} & \dfrac{q_{22}}{\hat{R}} \end{bmatrix} \begin{bmatrix} \hat{\varphi}_{\text{tar}} - \hat{\varphi}_{\text{int}} \\ \hat{\omega}_{\text{tar}} - \hat{\omega}_{\text{int}} \end{bmatrix} - \begin{bmatrix} g_{11} & g_{12} \\ g_{21} & g_{22} \end{bmatrix} \begin{bmatrix} 0 \\ \left(\dfrac{1}{T_{\text{int}}} - \dfrac{2\hat{\dot{R}}}{\hat{R}} \right) \hat{\omega}_{\text{tar}} \end{bmatrix} \right]$$

$$= \begin{bmatrix} 0 & \dfrac{b}{k_{\text{j}} T_{\text{int}}} \end{bmatrix} \begin{bmatrix} \dfrac{q_{11}}{\hat{R}} \Delta\hat{\varphi} + q_{12}\Delta\hat{\omega} - g_{12} \left(\dfrac{1}{T_{\text{int}}} - \dfrac{2\hat{\dot{R}}}{\hat{R}} \right) \hat{\omega}_{\text{tar}} \\ q_{21}\Delta\hat{\varphi} + \dfrac{q_{22}}{\hat{R}} \Delta\hat{\omega} - g_{22} \left(\dfrac{1}{T_{\text{int}}} - \dfrac{2\hat{\dot{R}}}{\hat{R}} \right) \hat{\omega}_{\text{tar}} \end{bmatrix},$$

then

$$\jmath_{\text{int}} = \frac{bq_{21}}{k_{\text{j}} T_{\text{int}}} \Delta\hat{\varphi} + \frac{bq_{22}}{k_{\text{j}} T_{\text{int}} \hat{R}} \Delta\hat{\omega} - \frac{bg_{22}}{k_{\text{j}} T_{\text{int}}} \left(\frac{1}{T_{\text{int}}} - \frac{2\hat{\dot{R}}}{\hat{R}} \right) \hat{\omega}_{\text{tar}}, \qquad \Delta\hat{\varphi} = \hat{\varphi}_{\text{tar}} - \hat{\varphi}_{\text{int}}, \quad \Delta\hat{\omega} = \hat{\omega}_{\text{tar}} - \hat{\omega}_{\text{int}}. \tag{13}$$

Direct analysis of (13) allows us to conclude the following:

1. The control signal (13) is all-altitude. This property is ensured by using the interceptor's lateral acceleration, instead of the rudder deflection angle, as the control signal; recall that the rudder's efficiency depends on air density, which varies with altitude.

2. The control signal consists of three components, with the first term $\frac{bq_{21}}{k_{\text{j}} T_{\text{int}}}\Delta\hat{\varphi}$ representing a modification of the direct method, and the sum of the first and second terms $\frac{bq_{21}}{k_{\text{j}} T_{\text{int}}}\Delta\hat{\varphi} + \frac{bq_{22}}{k_{\text{j}} T_{\text{int}} \hat{R}}\Delta\hat{\omega}$ representing the method of sequential predictions. At long ranges as $\hat{\omega}_{\text{tar}} \to 0$ and $\frac{bq_{22}}{k_{\text{j}} T_{\text{int}} \hat{R}} \to 0$, the requirement to eliminate the angle errors $\Delta\varphi$ becomes most significant. At short ranges, along with the growing influence of the second term due to an increase of $\frac{bq_{22}}{k_{\text{j}} T_{\text{int}} \hat{R}}$ for smaller R, the significance of the third term also raises with increasing $\hat{\omega}_{\text{tar}}$. Therefore, the control signal is time-varying. The factor $\frac{1}{T_{\text{int}}} - \frac{2\dot{R}}{R}$ in the third term of (13), which characterizes the mismatch between the dynamic properties of the interceptor and HSA, actually account for this mismatch in the control signal. It increases for short ranges, predetermining the growing influence of the target's maneuver. Since the mismatch between the dynamic properties of the interceptor and HSA is included in the control signal, it can be compensated for by generating an appropriate control action.

3. To form the required control signal (13), it is necessary to estimate the range, approach speed, onboard bearing of the HSA, and the LoS angular rate, which imposes no restrictions on its practical realization.

4. The weight of errors in the control signal (13) is determined not by the absolute values of the penalty coefficients, but by their ratios $\frac{q_{21}}{k_{\text{j}}}$, $\frac{q_{22}}{k_{\text{j}}}$, and $\frac{g_{22}}{k_{\text{j}}}$.

3. EFFICIENCY ANALYSIS OF THE CONTROL SIGNAL

Computer simulations are intended to verify the potential feasibility of intercepting a complexly maneuvering HSA, with a change in the sign of the angular rate derivative, using an inertial interceptor with the control law (13).

The simulations were carried out for HSA interception on head-on crossing courses, provided that the target is faster than the interceptor, with a limitation on the magnitude of the control

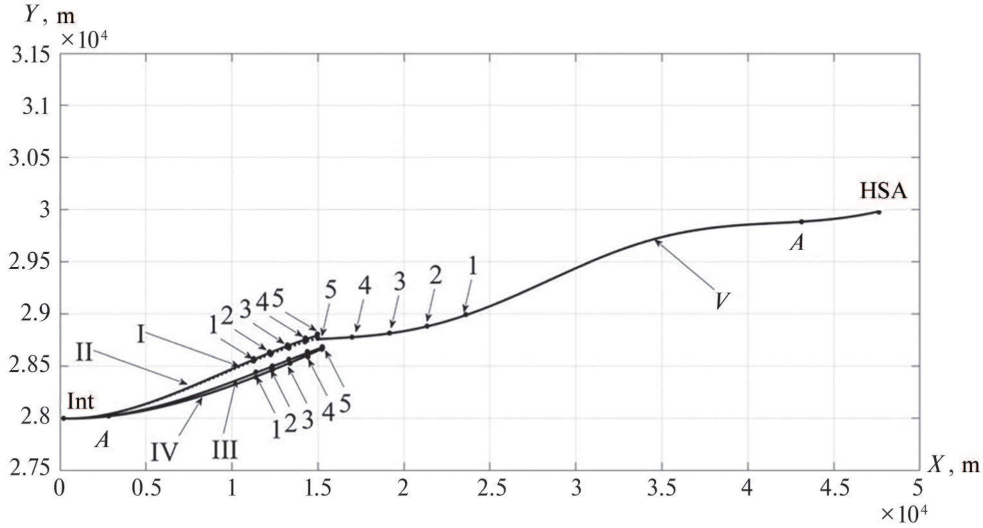

Fig. 2. Trajectories of HSA and interceptor during the interception process.

signal and without estimation errors, i.e., $\hat{R} = R$, $\hat{\dot{R}} = \dot{R}$, $\hat{\varphi}_{\text{tar}} = \varphi_{\text{tar}}$, $\hat{\varphi}_{\text{int}} = \varphi_{\text{int}}$, $\hat{\omega}_{\text{tar}} = \omega_{\text{tar}}$, and $\hat{\omega}_{\text{int}} = \omega_{\text{int}}$. This assumption is valid since the desired control signal ensures a potential interception (in the absence of noise and disturbances). When implementing this approach, the dynamic errors of the guidance system can be preliminarily estimated, in the form of current and final miss distances, from the simulation results. The estimation of fluctuation errors, when the noises are nonzero, requires additional studies.

To assess the possibility of simplifying the control law (13), we tested three schemes of the guidance law:

scheme I, defined by the relation (13);

scheme II, defined by the relation

$$\hat{j}_{\text{int}} = \frac{bq_{21}}{k_{\text{j}}T_{\text{int}}}\Delta\hat{\varphi} + \frac{bq_{22}}{k_{\text{j}}T_{\text{int}}\hat{R}}\Delta\hat{\omega}; \tag{14}$$

scheme III, defined by the relation

$$\hat{j}_{\text{int}} = \frac{bq_{21}}{k_{\text{j}}T_{\text{int}}}\Delta\hat{\varphi} \tag{15}$$

(under different values of the interceptor's time constant T_{int}).

The efficiency was assessed by the current and final miss distances, as well as the interceptor's lateral accelerations realized during the interception process.

The simulation results are shown in Figs. 2–5, namely:

—the motion of the HSA and interceptor along the entire interception trajectory in the vertical plane (Fig. 2);

—the trajectories of the HSA and interceptor at the final guidance stage (Fig. 3);

—the current h and final h_{fin} miss distances realized in the guidance schemes j_1, j_2, and j_3 (Fig. 4);

—the realized lateral accelerations (Fig. 5).

In Figs. 2 and 3 for the vertical plane XOY, numerals I, II, and III denote the interceptor's trajectories when realizing the guidance schemes j_1, j_2, and j_3, respectively, for a time constant of

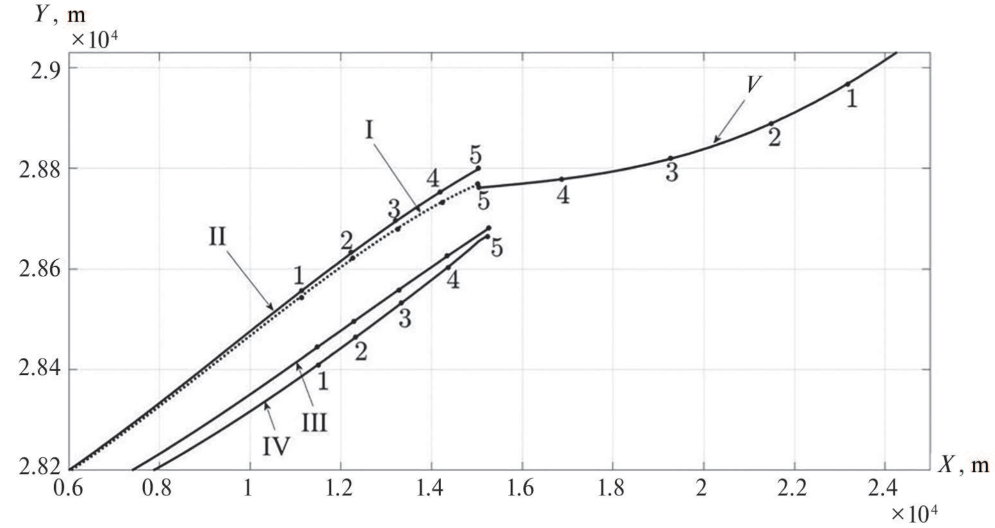

Fig. 3. Trajectories of HSA and interceptor at the final guidance stage.

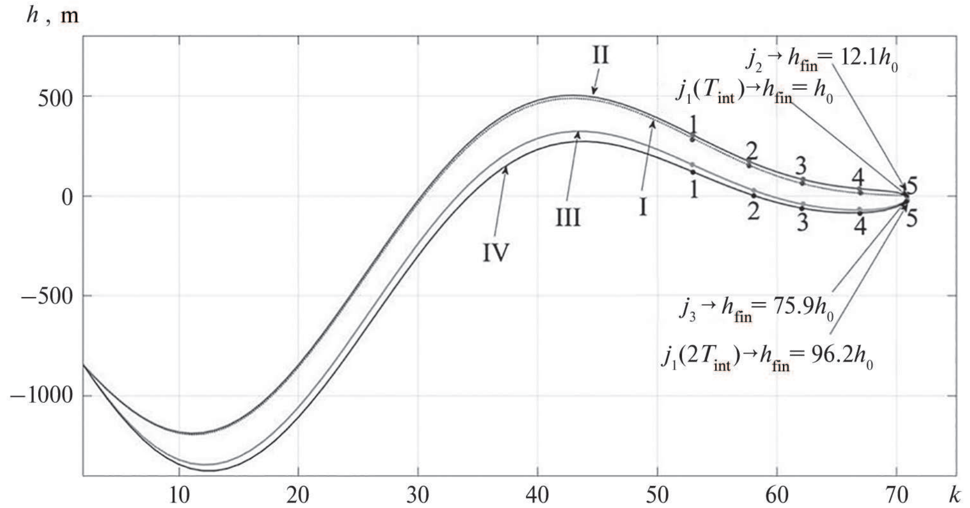

Fig. 4. The current and final miss distances of the interceptor with different guidance laws.

$T_{\rm int} = 2$ and $b = 2$; the numeral IV corresponds to the interceptor's trajectory when realizing the guidance scheme j_1 for a time constant of $2\,T_{\rm int}$; V indicates the trajectory of the maneuvering HSA with a change in the sign of the derivatives of the state coordinates; points HSA and Int are the initial positions of the HSA and interceptor, respectively; finally, points A, 1, 2, 3, 4, and 5 are the current positions of the HSA and interceptor at the same time instants.

In Fig. 4, curves I–IV are the current miss distances h when realizing the guidance schemes j_1, j_2, and j_3; $h_{\rm fin}$ is the final miss distance; finally, h_0 is the final miss distance when realizing the guidance scheme j_1 for a time constant $T_{\rm int}$.

In Fig. 5, curves I–IV are the current lateral accelerations arising during the interception process.

Direct analysis of the simulation results leads to the following conclusions:

1. The time-varying control law j_1 (13), which takes into account the mismatch between the dynamic properties of the target and interceptor, improves the guidance accuracy of the inertial interceptor. At the same time, an attempt to simplify the control law by using the lateral acceler-

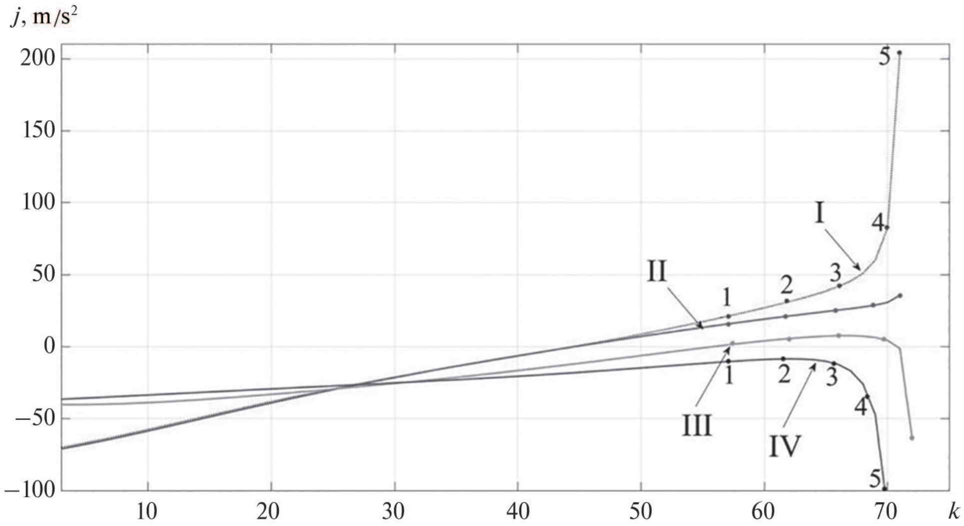

Fig. 5. The lateral accelerations of the interceptor with different guidance laws.

ations (14) and (15) decreases the guidance accuracy, in terms of the final miss distance h_{fin} of the interceptor (see curves I–IV in Fig. 4).

2. The time-varying nature of the guidance law is significant for guidance efficiency. This is confirmed by curves I–III in Fig. 2. According to the analysis, the time-varying guidance laws along trajectories I and II with the above initial conditions, after the interceptor covers the first 3 km (point A in Fig. 2, about 40 km to the target), are separated from curve III, which is the result of interception by the time-invariant guidance law.

3. The additional consideration of the mismatch between the dynamic properties of the interceptor and target in the law j_1 has an effect at the final interception stage. When the interceptor passes the mark of about 7 km, trajectories I and II in Fig. 3 are separated. This interceptor position corresponds to a range of about 25 km to the target. Therefore, it is crucial to account for the mismatch between the dynamic properties of the interceptor and target in the guidance law.

4. The current miss distances are convergent for all interceptor control laws j_1–j_3, as evidenced by the joint analysis of curves I–IV in Fig. 4.

5. Doubling the interceptor's inertia, characterized by the time constant T_{int}, reduces the interception efficiency, as evidenced by the joint analysis of curves I and IV in all figures.

6. There are no restrictions on the practical realization of the control law (13). Indeed, on the one hand, the existing range, speed, and angular coordinate sensors can be used for the information support of (13); on the other, guidance is performed within realizable lateral accelerations (curves I–IV in Fig. 5).

4. CONCLUSIONS

In this paper, based on the local optimization approach of the statistical theory of optimal control, a time-varying control law for an inertial interceptor's guidance to an intensively maneuvering aerial target has been designed. This law takes into account the mismatch between the dynamic properties of the interceptor and the target.

Due to the time-varying nature of the control law and consideration of the mismatch between the dynamic properties of the interceptor and target, the final miss distance of the interceptor has been reduced. At the same time, in the above simulation conditions, the time-varying control law has an effect starting from a range of about 40 km to the target; consideration of the mismatch between the dynamic properties of the interceptor and target, starting from a range of about 25 km to the target.

The time-varying property of the guidance law has been ensured by introducing time-varying penalty coefficients for control accuracy (depending on the application conditions) into the performance functional. The mismatch between the dynamic properties of the interceptor and HSA has been taken into account by using different mathematical models of the objects and by introducing the matrix of measured disturbances (characterizing the above mismatch) into the performance functional.

It has been established that the time-varying interceptor control law, which considers the mismatch between the dynamic properties of the interceptor and the target, potentially ensures an interception of the target.

REFERENCES

1. Verba, V.S., Merkulov, V.I., and Zakomoldin, D.V., Problems of Interception of High Speed Aircraft Maneuvering According to Complex Laws. Part 1. Features of the Use of High Speed Aircraft, Complicating Their Interception, *Achievements of Modern Radioelectronics*, 2024, vol. 78, no. 3, pp. 5–12.
2. Verba, V.S., Merkulov, V.I., Zakomoldin, D.V., and Likhachev, V.P., Problems of Interception of High Speed Aircraft Maneuvering According to Complex Laws. Part 2. Analysis of Flight Paths of Foreign Aircraft, *Achievements of Modern Radioelectronics*, 2024, vol. 78, no. 4, pp. 5–14.
3. Yibo, D., Yue, X., Chen, G., et al., Review of Control and Guidance Technology on Hypersonic Vehicle, *Chinese Journal of Aeronautics*, 2022, vol. 35, no. 7, pp. 1–18.
4. Grant, M. and Antony, T., Rapid Indirect Trajectory Optimization of a Hypothetical Long Range Weapon System, *Proceedings of the AIAA Atmospheric Flight Mechanics Conference*, 2016, pp. 1–19.
5. Besser, H., Shaffer, A., Zimper, D., et al., Hypersonic Vehicles: Game Changers for Future Warfare, *Transforming Joint Air Power: J. JAPCC*, 2017, no. 24, pp. 11–27.
6. Shen, H., Liu, Y., Chen, B., et al., Control-Relevant Modeling and Performance Limitation Analysis for Flexible Air-Breathing Hyper-Sonic Vehicles, *Aerospace Science Technology*, 2018, no. 76, pp. 340–349.
7. Karako, T. and Dahlgren, M., Complex Air Defense Countering the Hypersonic Missile Threat, *A Report of the CSIS Missile Defense Project*, 2022.
8. Verba, V.S., Merkulov, V.I., and Ilchuk, A.R., Approaches to Optimizing Guidance Methods to High-Speed Intensively Maneuvering Targets. Part III. Guidance Optimization Considering the Dynamic Properties of Interceptors, *Autom. Remote Control*, 2025, vol. 86, no. 2, pp. 153–164.
9. Merkulov, V.I. and Verba, V.S., *Sintez i analiz aviatsionnykh radioelektronnykh sistem upravleniya. Kniga 1* (Design and Analysis of Aircraft Radioelectronic Control Systems. Book 1), Moscow: Radiotekhnika, 2023.

This paper was recommended for publication by A.A. Galyaev, a member of the Editorial Board